sustainability

MDPI

Article

Valorization of MSWI Bottom Ash as a Function of Particle Size Distribution, Using Steam Washing

Enrico Destefanis [1], Caterina Caviglia [1,*], Davide Bernasconi [1], Erica Bicchi [2], Renato Boero [3], Costanza Bonadiman [4], Giorgia Confalonieri [5], Ingrid Corazzari [6], Giuseppe Mandrone [7], Linda Pastero [1], Alessandro Pavese [1], Francesco Turci [6] and Quentin Wehrung [2]

1 Earth Sciences Department, University of Turin, 10125 Turin, Italy; enrico.destefanis@unito.it (E.D.); davide.bernasconi@unito.it (D.B.); linda.pastero@unito.it (L.P.); alessandro.pavese@unito.it (A.P.)
2 ESAIP Engineer School, 49124 Saint-Barthélemy d'Anjou, France; ebicchi@esaip.org (E.B.); qwehrung.ing2020@esaip.org (Q.W.)
3 IREN S.p.A., 10143 Turin, Italy; Renato.Boero@gruppoiren.it
4 Earth Science and Physics Department, 44122 Ferrara, Italy; costanza.bonadiman@unife.it
5 Chemical and Geological Science Department, University of Modena and Reggio Emilia, 41125 Modena, Italy; giorgia.confalonieri@unimore.it
6 Department of Chemistry, University of Turin, 10125 Turin, Italy; ingrid.corazzari@unito.it (I.C.); francesco.turci@unito.it (F.T.)
7 Interuniversity Department of Regional and Urban Studies and Planning, 10125 Turin, Italy; giuseppe.mandrone@unito.it
* Correspondence: caterina.caviglia@unito.it

Received: 7 October 2020; Accepted: 9 November 2020; Published: 13 November 2020

Abstract: Treatments to reduce the leaching of contaminants (chloride, sulfate, heavy metals) into the environment from bottom ash (BA) are investigated, as a function of the ash's particle size (s). The aim is to make BA suitable for reuse as secondary raw material, in accordance with the legal requirements. Such treatments must be economically feasible and, possibly, have to use by-products of the plant (in this case, steam in excess from the turbine). For the sake of completeness and comparison, carbonation is performed on those BA particle size classes that are not positively responsive to steam washing. BA is partitioned into four different particle size classes ($s \geq 4.75$, $4.75 > s \geq 2$, $2 > s \geq 1$ and $s < 1$ mm, corresponding to 36, 24, 13 and 27 wt%, respectively). In the case of $s \geq 2$ mm (60 wt%), steam washing is effective in reducing to under the legal limits the leaching of chlorides, sulfate and heavy metals (Zn, Cu, Cd, Pb). It has been observed that steam washing causes both removal and dissolution of thin dust adherent to the BA's surface. BA with $2 > s \geq 1$ (~13 wt% of total BA) requires a combination of steam washing and carbonation to achieve a leaching below the legal limits. The finest BA fraction, $s < 1$ mm (~27 wt% of total BA), is treated by carbonation, which reduces heavy metals leaching by 85%, but it fails to sufficiently curb chlorides and sulfates.

Keywords: MSWI bottom ash; particle size; steam washing; carbonation

1. Introduction

Bottom ash (BA) is the main solid residue from municipal solid waste incineration and represents about 20–25 wt% of the whole burnt waste [1]. BA's bulk chemical and phase compositions are heterogeneous [2], as both depend on the particle size (s) distribution, which ranges from a few μm to more than 100 mm. The coarser fractions ($s > 4$ mm) are principally composed of fragments of glass, metals and ceramic materials, as already observed in [3–6]. The incineration process produces a solid residue bearing a variety of contaminant species (i.e., chlorides and toxic metals), which lead BA to be

often classified as dangerous waste [7,8]. For this reason, in several European countries (for instance: Denmark, the Netherlands, France) BA is subject to treatments to reduce its toxic species leaching into the environment and reuse it as secondary raw material to replace aggregates [9].

A variety of treatments have been designed, even as a function of particle size, to reduce the BA's leaching of contaminants, such as chlorides, sulfates and heavy metals. Among the most common treatments there are: (i) stabilization with cement [10,11]; (ii) thermal treatments and vitrification [12–14]; (iii) washing with water [15–17]; (iv) natural carbonation, or aging [18]. Washing with water-based solutions (largely adopted in the Netherlands), in combination with physical separation as a function of the particle size, is very effective in removing water-soluble salts and reducing the concentration of heavy metals and organic matter [15–17,19–21]. Metals, in turn, can be physically separated and recovered from untreated BA > 0.5 mm by means of eddy currents and ballistic separation methods [22–24]. The present study is a contribution towards designing, at laboratory scale, a treatment process to recover as large a BA amount as possible by exploiting steam ("steam washing"). The study employs the BA from the latest generation municipal solid waste incineration plant of Turin (Northern Italy). The aim is to reduce the contaminant leaching from BA to below the Italian legal limit values that are set for using ash in geotechnical applications. In doing so, the dependence of BA on its particle size (s) is exploited. Carbonation treatments in a regime of CO_2-saturation and P ~2 bar, are employed for those BA particle size classes for which steam washing is not effective, for reason of completeness and comparison.

Two reasons underpin the interest in steam washing:

(1) high flexibility in terms of treatment conditions, in particular: working temperature and combination of steam with gases;

(2) benefits to the operational, economic and environmental sustainability of the municipal solid waste incineration process, such as the development of flexible strategies that provide different ways of exploiting by-products such as steam, nowadays destined for electricity generation and domestic water warming.

2. Materials and Methods

BA was provided by the municipal solid waste incinerator of the metropolitan area of Turin (Northern Italy). It was sampled at the incineration plant after cooling, from a falling stream of wet material (see [25]), and successively quartered to obtain a representative sample of 20 kg (please, see for details: [26]). We determined the residual water content, ~17 %, measuring the difference by weight between pristine BA, and BA after drying at 105 °C for 24 hours. The loose bulk density, ~1.095 $Mg \cdot m^{-3}$, was determined by (i) filling a 500 mL cylindrical container with dried BA until they spilt over, and (ii) levelling the top surface by rolling a rod.

The BA's particle size distribution was measured by sieving, with openings from 1 to 4.75 mm (see Figure S1 in the Supplementary Material). Following [26], BA was partitioned as a function of s into four classes: $s \geq 4.75$, $4.75 > s \geq 2$, $2 > s \geq 1$ and $s < 1$ mm, corresponding to 36, 24, 13 and 27 wt%, respectively. Details about phase and chemical compositions of the BA under investigation are reported in [26]. The quoted paper shows that the main contaminants are sulfate, chloride, nitrate and heavy metals (Cu, Pb, Zn, Cr, Ni, Cd). As, Be, Se, Sb, V and fluoride lie under the legal limit values.

The effects induced by treatments on BA are characterized by means of: (a) Thermo-gravimetric Analyses (TGA), X-ray Powder Diffraction (XRPD), Scanning Electron Microscopy (SEM), Solid-State Nuclear Magnetic Resonance (SSNMR), for solid matrixes; (b) leaching tests in deionized water, for the determination of electrolytic conductivity, concentrations of heavy metals, chlorides, sulfates and nitrates. The chemical composition (major, minor and trace elements) of the leachates was determined by Inductively Coupled Plasma Mass Spectroscopy (ICP-MS).

2.1. Steam Washing

Laboratory steam washing experiments were carried out on BA using steam from deionized water (total balance: 0.02 L/kg/s), at P ~ 2 bar, T ~ 80 °C and exploring treatment times from 60 to 600 secs.

These conditions, which do not correspond to an equilibrium regime of steam, are compatible with a steam flux from turbines and allow for the recovery of a considerable fraction of thermal energy. Steam washing as a function of its working conditions will be discussed elsewhere; we focus here on the general principle and its efficacy to treat BA. A steam generator prototype designed by ETG s.r.l, in collaboration with the Earth Science Department of the University of Turin, was employed. A steam flow, conveyed through a pipe, is released by a nozzle and directed onto a BA sample (30–40 g) laid on a grid, under which condensation water is then collected. The process takes place without restraining walls, to avoid steam oversaturation. The steam's temperature is measured by an E + E Elektronik EE 33 sensor (operating range −40 °C < T < 180 °C, 0 < Hr <100%; accuracy for T and Hr: ±0.2 ° C and Hr = ±1.3%, respectively). The flow is determined through an E + E Elektronik EE 75 flow sensor that measures the gas velocity (sensitivity range: 0 < V < 40 m/s; accuracy: from 0.06 m/s to 2 m/s; operating conditions: −40 < T < 120 °C, maximum pressure ~10 bar) and provides a pressure estimate by Bernoulli's equation.

2.2. Carbonation

Carbonation takes place mainly via the following net reaction:

$$MO(s) + CO_2 \rightarrow MCO_3$$

where M is a divalent cation, in particular Ca^{2+}. More complex reactions occur as a function of the available chemical species and chemical-physical conditions (pH, P_{CO_2}, T). The laboratory reactor used in the present investigation for CO_2 treatments was purposely designed and assembled by Maina G. s.r.l.

CO_2 was provided by a gas tank and its pressure was gauged via a manometer at the reactor. Experiments were carried out in "closed system mode," as follows: (1) the system was warmed to a given temperature by a H_2O-thermal reservoir surrounding the reactor and heated by a coiling resistance; (2) temperature was measured in the reservoir and inside the reactor by a thermocouple; (3) a feedback control system made it possible to keep the temperature constant in the reactor; (4) carbon dioxide was allowed to flow in until the chosen pressure was achieved; (5) the system was isolated, so that any in/out CO_2 exchange was prevented and carbonation occurred.

The parameters used in carbonation experiments (T < 60–80 °C; duration of carbonation: $t \leq$ 180 min; $P_{CO_2} \leq$ 2–3 bar; CO_2-saturation) are in keeping with those of previous works [27–31]. The liquid (i.e., water)-to-solid (i.e., BA) ratio was set in the range 0.2–0.4, to promote mobilization of ions for carbonic acid formation and interaction with alkaline/alkaline-earth metals. Low temperature carbonation reactions at 6 °C were performed by cooling the reactor's outside walls with cold water.

2.3. X-ray Powder Diffraction

X-ray Powder Diffraction was used for phase composition determination. The samples were first dried for 24 h in an oven, then manually ground (<30 μm) to minimize preferred orientation effects. XRPD data collection was performed by a PANalytica lX'Pert Pro Bragg Brentano (θ/2θ) diffractometer, using Cu-Kα incident radiation and operating at 40 kV–40 mA. The diffractometer was equipped with an X'Celerator detector and an optic configuration consisting of a fixed divergence slit (1/2°) and anti-scatter slit (1/2°). Samples were rotated at 16 rpm and patterns were collected between 5° and 80° 2θ-angle, with a 2θ-step size of 0.017°. The amorphous phase quantification was carried out by combining Rietveld and reference intensity ratio (RIR) methods [32]. High purity calcined α-Al_2O_3 corundum was used as an internal standard and added to the ground samples (10 wt%). Data refinements were performed by the software GSASII [33].

2.4. Optical Microscopy

A stereomicroscope trinocular Optika SZO-4 (Optika Microscopes, Ponteranica, Italy) with achromatic zoom 0.67–4.5 × and additional lens 2 × (zoom factor 6.72:1) was used to examine the surface of the bottom ash, before and after steam washing treatment.

2.5. Scanning Electron Microscope (SEM-EDS)

Back scattered electrons (BSE) images and analyses were performed by a Scanning Electron Microscope JSM IT300LV High Vacuum – Low Vacuum 10/650 Pa – 0.3–30 kV (JEOL USA Inc., Peabody, MA, USA), equipped with SE and BSE detectors (typical experimental conditions: W filament, EHT 10 kV, working distance 10 mm, standard probe current). The analyses were performed in low vacuum mode with non-coated samples of carbonated BA, to evaluate the carbon distribution over the surface, due to the carbonation process. Regarding the other samples, graphite coating and high vacuum mode were employed.

2.6. Leaching Tests

Leaching tests were carried out following the European standard for characterization of waste [34–36]: (1) EN-12457-2, i.e., a leaching test in deionized water for particles with $s < 4$ mm, with a Liquid-to-Solid ratio of 10/1; (2) EN-12457-4, i.e., a leaching tests in deionized water for particles of $s < 10$ mm, and a ratio L/S 10/1. Leachates were analysed in terms of anions (Cl^-, SO_4^{2-}, NO_3^-), alkaline/alkaline-earth cations (Na^+, K^+, Ca^{2+}) and heavy metals (As, Ba, Be, Se, Cu, Zn, Ni, Pb, Cr, Cd, Co, V) concentrations by means of:

(i) Ion chromatography, using a Metrohm 883 IC plus instrument with a loop of 20 ml, equipped with a column MetroSep A Supp 7 250/4.0, for anions, and a column Metrosep C4 250/4.0, for cations. Calibration was performed by eight analysis points on a reference sample (detection limit: ~10 µg/L);

(ii) ICP-MS Spectroscopy, using a Perkin Elmer Optima 2000 DV and applying a calibration curve determined by four points using a Merck ICP multi-element standard solution IV (detection limit: ~1 ppb µg/L).

Leaching tests on BA samples were carried out before and after treatments, to compare the chemical species' concentrations in the leachates with the legal limits for waste reuse, according to the Italian Ministerial Decree 186/2006 (see reference list [37]).

2.7. PHREEQC Modelling

Wastewater solutions, resulting from steam condensation and subsequent percolation through BA, were modelled by calculating the saturation indices (SI) of the possible mineral phases that might precipitate, using the PHREEQC with MINTEQ v.4 database [38]. The measured composition of the major cations and anions and pH were provided as input.

2.8. Thermogravimetry (TGA)–Fourier Transform Infrared Spectroscopy (FTIR) Analysis

TGA curves of treated versus untreated samples allowed the determination of sequestered CO_2. About 10 mg of material was placed in a Pt crucible and heated from 30 to 900 °C (heating rate of 20 °C/min) under dynamic inert atmosphere (N_2 100%, flow rate: 35 mL min^{-1}) in a Pyris 1 TG analyzer (PerkinElmer, Waltham, MA, USA). The gas evolved upon heating was piped (gas flow 65 mL min^{-1}) via a pressurized heated (280 °C) transfer line (Redshift S.r.l., Vicenza, Italy) and analyzed continuously by a FTIR spectrophotometer (Spectrum 100, PerkinElmer), equipped with a thermostatic conventional gas cell. Time-resolved spectra were collected in the 4000–600 cm^{-1} wavenumber range with a resolution of 0.4 cm^{-1} and analyzed with the Spectrum software (PerkinElmer) to identify the nature of volatiles. Infrared profiles, of each single species desorbed from the samples, were obtained as a function of temperature from the representative peak intensity of the investigated species.

2.9. Solid-State Nuclear Magnetic Resonance Spectroscopy (SSNMR)

^{13}C MAS SSNMR spectroscopy allowed insights into the mechanism of carbon dioxide capture. ^{13}C MAS spectra were recorded by a Jeol ECZR 600 instrument, operating at 600.17 and 150.91 MHz,

respectively, for ^{1}H and ^{13}C nuclei. Sample preparation was as follows: (1) the ferromagnetic fraction was manually removed by a magnet from 5 g of BA with $s < 1$ mm; (2) the remaining portion was desiccated and further manually ground; (3) the powders were packed into a cylindrical zirconia rotor with a 3.2 mm o.d. and a 60 µL volume. ^{13}C MAS spectra were collected at a spinning speed of 20 kHz, using a recycle delay of 20 s and a number of scans in the range 1100–3100, as a function of the sample. A ^{13}C 90° pulse of 2 µs was employed. A two-pulse phase modulation (TPPM) decoupling scheme was used, with a radiofrequency field of 108.5 kHz. The ^{13}C chemical shift scale was calibrated by the methylene signal of an external standard glycine (at 43.5 ppm).

3. Results and Discussion

The reported results are the averages of sequences of independent measurements (both treatments and related analyses were repeated) on solid fractions and leachates. A sequence achieves convergence when the last three observations agree with each other within 30% (see [39,40]). Note that every individual measurement of the contaminants in the leachates from BA was repeated 10–15 times.

3.1. Steam Washing

3.1.1. Leaching Reduction

The electrolytic conductivity of the leachates from steam washed BA ($s \geq 4.75$ mm) decreases as a function of the treatment time (see Figure S2 in the Supplementary Material). This provides an indication about the residual soluble fraction of the treated BA, which are responsible for the presence of free charge carriers in the solution. The electrolytic conductivity achieves a steady value over 180 s, thus suggesting that the efficacy of the steam washing treatment does not increase monotonically with time. The results related to the leaching tests on BA ($s \geq 4.75$ mm) as a function of the steam washing treatment time are shown in Figure 1 for the main contaminants.

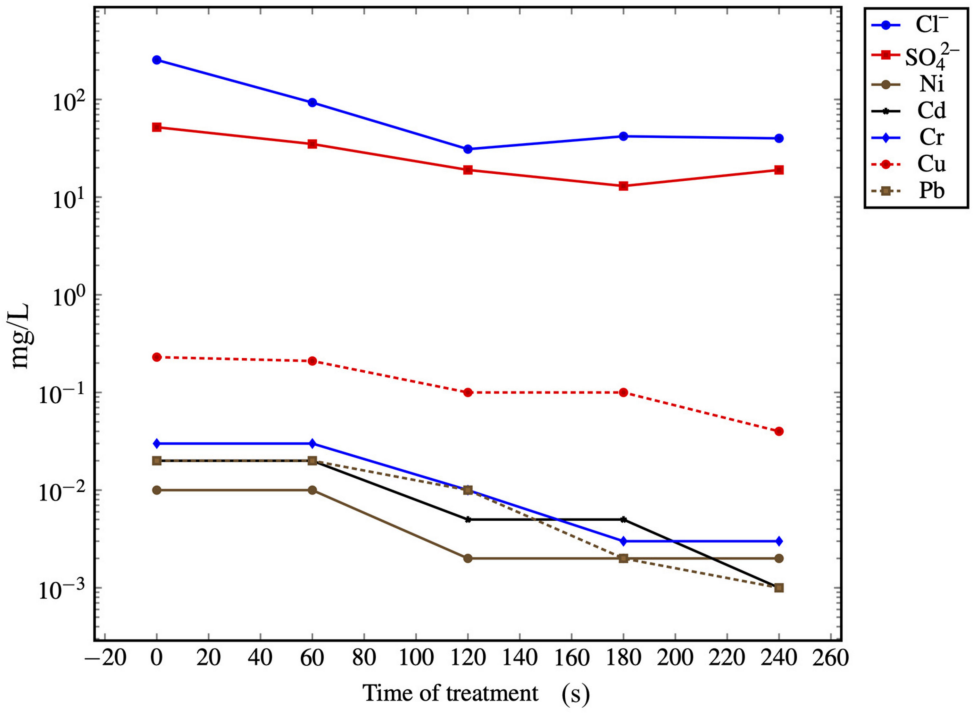

Figure 1. Concentrations (mg/L, log scale) versus treatment time of the main pollutants after steam washing on bottom ash (BA) with $s \geq 4.75$ mm.

Table 1 reports the main pollutant concentrations observed in leachates from BA ($s \geq 4.75$ mm) after a steam washing duration of 240 s, i.e., once the steam washing treatment has fully achieved its maximum cleaning capacity for the particle size class under study.

Table 1. Analyses of leaching tests of BA ($s \geq 4.75$ mm) untreated and treated by steam washing for 240 s, and comparison with Italian legal limits for reuse (Min. Dec. 186/2006). Standard deviations are reported. F^-, Be, V, As, Se are not set out, as they lie below the detection limits. All concentration values are expressed in mg/L. LOQ for Cd and Co is 0.0005 µg/L.

	Cl^-	SO_4^{2-}	NO_3^-	Ni	Zn	Ba	Cd	Co	Cr	Cu	Pb
$s \geq 4.75$ mm, untreated											
Average	257	54.3	0.52	0.015	0.029	0.02	0.017	0.0397	0.027	0.3	0.03
St. Dev.	6.4	2.51	0.15	0.005	0.018	0.005	0.008	0.0107	0.013	0.024	0.016
$s \geq 4.75$ mm, 240 s											
Average	40	19.7	0.25	0.002	0.001	0.003	<LOQ	<LOQ	0.002	0.024	0.003
St. Dev.	4.6	2.13	0.2	0.001	0.0003	0.002	<LOQ	<LOQ	0.002	0.015	0.002
Italian legal limit values (mg/L)	100	250	50	0.01	3	1	0.005	0.25	0.05	0.05	0.05

A 60 s steam washing can partially remove the fine dust deposited on the surface of the particles and efficiently solubilize species like chlorides and some sulfates, whose concentrations lie significantly above the legal limit values in the pristine material. Increasing the steam washing duration significantly improves the removal of chlorides, sulfates and Cu: a 120 s treatment yields a Cu reduction of 50%, though copper still remains over the legal limit value (0.1 mg/L against 0.05 mg/L), whereas Cd and Ni are removed. After 240 s steam washing, Cu also lies under the legal limit value, along with the other measured heavy metals. Increasing the steam washing time provides a further reduction of Cu, although at the cost of excessive steam usage.

BA ($4.75 > s \geq 2$ mm) underwent steam washing up to 600 s, as shown in Figure 2. Among the heavy metals, the efficacy of the treatment duration on Cu and Cr is noticeable, passing from 300–400 to 600 s.

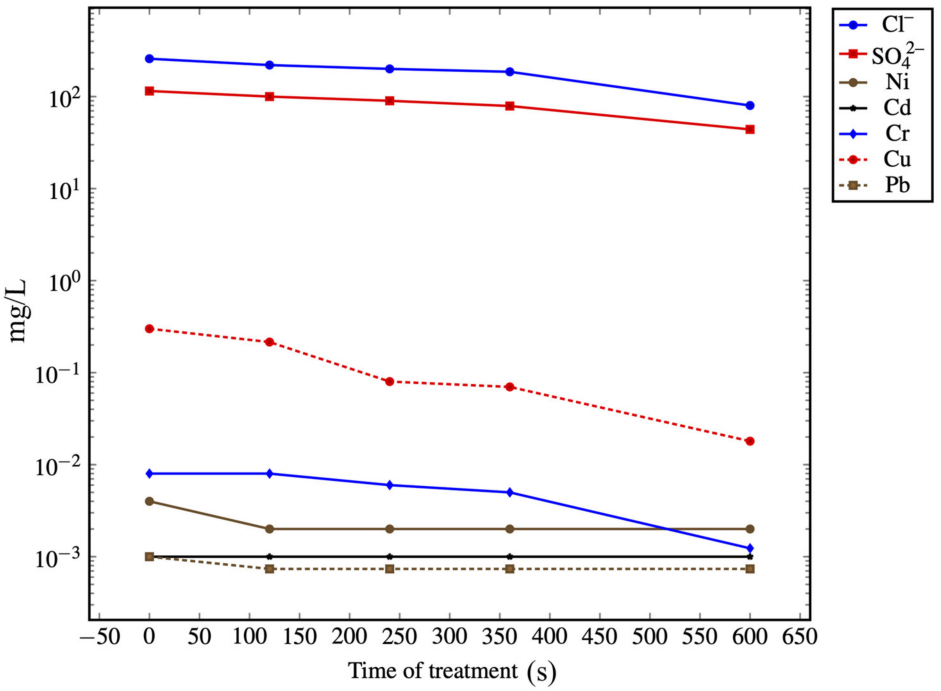

Figure 2. Concentrations (mg/L, log scale) versus treatment time of the main pollutants after steam washing on BA with $4.75 > s \geq 2$ mm.

Table 2 reports the case of a treatment time of 600 s. A comparison between unwashed and washed material shows that chlorides, sulfates, Cd, Cr and Cu are reduced below the legal limit values.

Table 2. Results of the leaching tests of BA ($4.75 > s \geq 2$ mm), untreated and treated by steam washing for 600 s, and comparison with Italian legal limits for reuse (Min. Dec. 186/2006). Standard deviations are reported. F^-, Be, V, As, Se are not set out, as they lie below the detection limits. All concentration values are expressed in mg/L.

	Cl^-	SO_4^{2-}	NO_3^-	Ni	Zn	Ba	Cd	Co	Cr	Cu	Pb
$4.75 > s \geq 2$ mm, untreated											
Average	252	115	0.4	0.004	0.013	0.005	0.001	0.005	0.007	0.27	0.001
St. Dev	21.4	8.15	0.1	0.001	0.002	0.002	0.001	0.001	0.001	0.048	0.002
$4.75 > s \geq 2$ mm, 600 s											
Average	82	44	0.2	0.002	0.003	0.001	0.001	0.002	0.004	0.045	0.001
St. Dev.	6.6	14.6	0.08	0.001	0.003	0.001	0.003	0.001	0.002	0.012	0.001
Italian legal limit values (mg/L)	100	250	50	0.01	3	1	0.005	0.25	0.05	0.05	0.05

The results for BA ($2 > s \geq 1$ mm) are displayed in Figure 3.

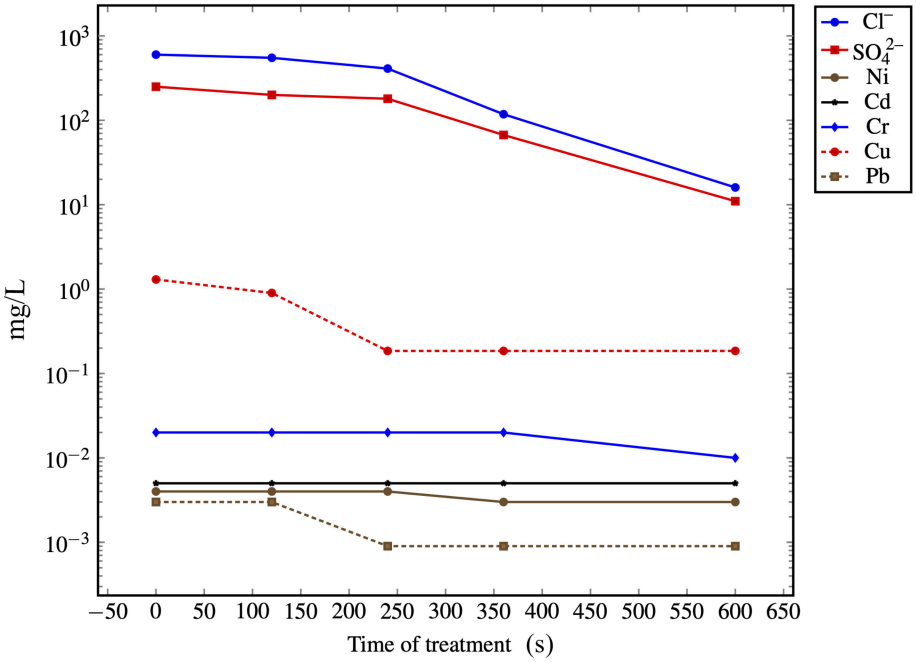

Figure 3. Concentrations (mg/L, log scale) versus treatment time of the main pollutants after steam washing on BA with $2 > s \geq 1$ mm.

Two aspects are worth highlighting: (i) Cl^- and SO_4^{2-} exhibit a monotonically decreasing trend and a quasi-linear dependence on time in the range 200–600 s. This yields a "measure" of the correlation between treatment efficacy and time for such species; (ii) Cu follows a flat trend from 200 to 600 s, thus suggesting that even an economically undesirable increase of the treatment time would not provide any significant improvement in terms of copper concentration reduction.

The leachates' compositions of the unwashed BA ($2 > s \geq 1$ mm) show Cu concentrations up to four times as large as those of the unwashed sample with $4.75 > s \geq 2$ mm, as reported in Table 3. Leaching tests prove that steam washing does lead to a relevant decrease of chlorides, sulfates and heavy metals like Cd and Cr, but it fails in reducing copper below the legal limit value, even with 600 s treatments.

Table 3. Results of leaching test of BA ($2 > s \geq 1$ mm) untreated and treated by steam washing for 600 s, and comparison with Italian legal limits for reuse (Min. Dec. 186/2006). Statistical data are reported. F^-, Be, V, As, Se are not reported, as they lie below the detection limits. All concentration values are expressed in mg/L.

	Cl^-	SO_4^{2-}	NO_3^-	Ni	Zn	Ba	Cd	Co	Cr	Cu	Pb
$2 > s \geq 1$ mm untreated											
Average	594	248	0.4	0.007	0.032	0.03	0.004	0.005	0.07	1.24	0.003
St. Dev.	18.5	3.5	0.08	0.001	0.003	0.01	0.001	0.003	0.02	0.13	0.001
$2 > s \geq 1$ mm, 600 s											
Average	16	11.8	0.2	0.004	0.01	0.03	0.001	0.002	0.05	0.07	0.001
St. Dev.	1.13	0.9	0.081	0.001	0.001	0.01	0.001	0.001	0.01	0.01	0.001
Italian legal limit values (mg/L)	100	250	50	0.01	3	1	0.005	0.25	0.05	0.05	0.05

3.1.2. Steam Washing Mechanism

In general, steam washing affects BA by a combination of mild dissolution and mechanical removal of the fine dust adherent to the surface of the particles. Figure 4a–f shows the BA before and after steam washing, for all grain sizes under study, using optical microscopy observations.

Small-size particles, adherent to the surface, are observable in untreated BA samples, whereas they are absent in samples that have undergone steam washing. An inspection of the particle edges brings to light rougher surfaces in untreated BA than treated samples. XRPD measurements of the dust covering untreated samples allowed us to observe the occurrence of an amorphous phase, low crystallinity Na-K-chloride, Ca-sulfates (anhydrite and gypsum), calcite and quartz, along with other minor phases (melilite, apatite). XRPD measurements on the solid residue of the wastewater from steam condensation and percolation though BA (we discuss this aspect below) prove the presence of the abovementioned phases, with the exception of NaCl, KCl, $CaSO_4$ and $CaSO_4$ $2H_2O$. Table 4 sets out the chemical composition of the wastewater. It shows that Na/K-chloride and Ca-sulfate underwent dissolution into water (pK_{sp} = −1.58, −0.85, and 4.36, respectively). This is further confirmed by observing the presence of Na^+, K^+ and Ca^{2+} (not shown in Table 4) to counterbalance Cl^- and SO_4^{2}.

Table 4. Wastewater composition of steam washing on BA with $s \geq 4.75$ mm, $4.75 > s \geq 2$ mm, $2 > s \geq 1$ mm (240, 600, 600 s). Be, V, As, Se and Hg are not reported, as they are below the detection limit. All concentration values are expressed in mg/L. LOQ for Cd, Co, Ba, Pb is 0.0005 µg/L, for Ni 0.002 µg/L.

Wastewater	Cl^-	SO_4^{2-}	NO_3^-	Ni	Zn	Ba	Cd	Co	Cr	Cu	Pb
$s \geq 4.75$ mm (240 s)											
Average	214	33	0.26	0.001	0.002	<LOQ	0.002	<LOQ	0.02	0.2	<LOQ
St. Dev.	16.26	6.66	0.02	0.001	0.001	<LOQ	0.001	<LOQ	0.01	0.01	<LOQ
$4.75 > s \geq 2$ mm (600 s)											
Average	150	51	0	0.001	0.01	<LOQ	< LOQ	<LOQ	0.003	0.3	<LOQ
St. Dev.	43.59	17.93	0	0.001	0.02	<LOQ	< LOQ	<LOQ	0.004	0.001	<LOQ
$2 > s \geq 1$ mm (600 s)											
Average	504	250	0.2	<LOQ	0.001	< LOQ	0.002	0.001	0.05	1.05	<LOQ
St. Dev.	53.95	0.83	0.01	<LOQ	0.001	< LOQ	0.001	0.001	0.03	0.001	<LOQ

PHREEQC modelling of the wastewater indicates a solution undersaturated with respect to NaCl, KCl, $CaSO_4$, and supersaturated in Ca-carbonates (calcite), Fe carbonates and Fe hydroxides, that can precipitate into the residual solid (Table S1 in the Supplementary Material). XRPD and SEM analyses of the solid residue confirm the presence of these phases, especially calcite, Fe oxides and hydroxides, apatite and quartz, together with slag phases. In addition, SEM observations yield an average particle size of the solid residue of about 700–800 µm, corroborating the removal of the fine fraction (BA with $s < 1$ mm) from the surface of coarser BA during treatment (Figure 5).

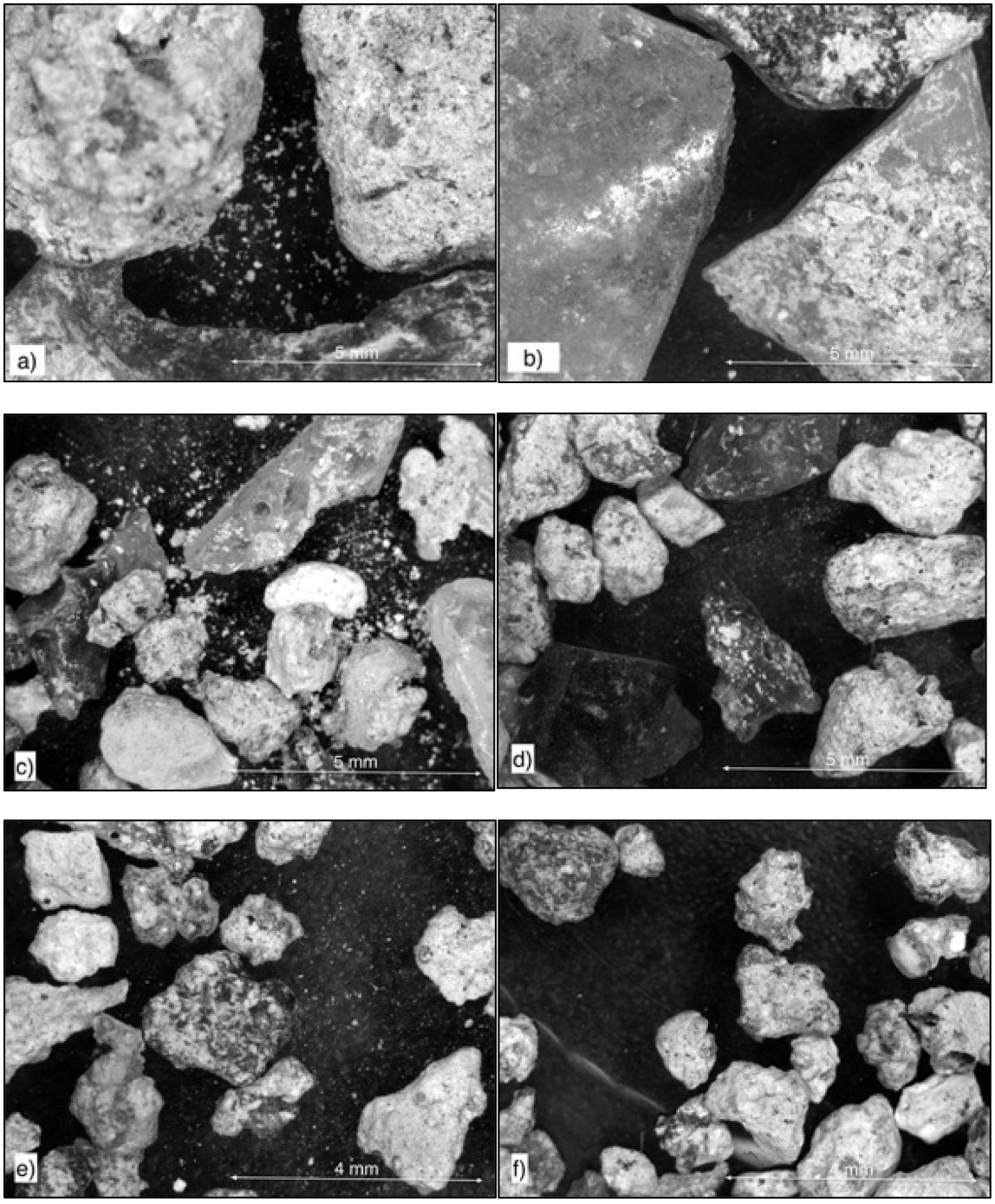

Figure 4. BA with $s \geq 4.75$ mm before (**a**) and after (**b**) steam washing; BA with $4.75 > s \geq 2$ mm before (**c**) and after (**d**) steam washing. Optical magnification 7.7×.; BA with $2 > s \geq 1$ mm before (**e**) and after (**f**) steam washing. Optical magnification 10 ×.

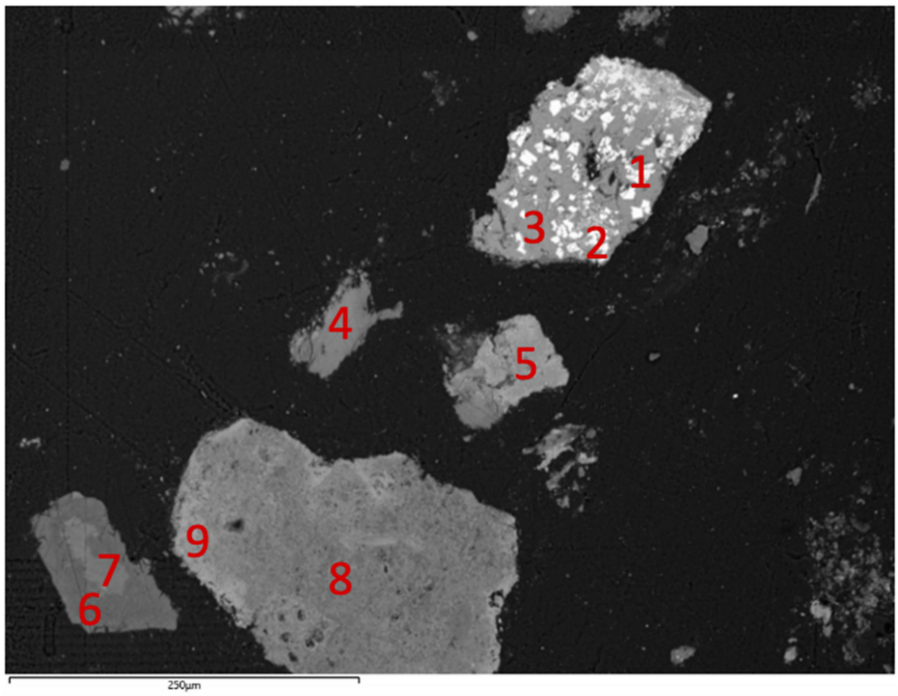

Figure 5. SEM images of solid residue removed during steam washing. SEM-EDS observations show a complex composition of both crystalline and slag phases (where no mineral could be identified the composition is reported in cement notation): 1. FeOx; 2. TiO_2; 3. Pyroxene; 4. Apatite; 5. CAS; 6. Mg-spinel; 7. CA.; 8. Calcite; 9. Quartz. (Experimental conditions: W filament, accelerating voltage 15 kV, working distance 10 mm, high probe current, magnification 200×).

The molar composition of the original BA, in terms of heavy metals, fulfills the following relationship: Zn > Cu > Cr > Cd > Pb. In the wastewater, the highest concentrations of heavy metals are provided by Cu, Cr, Zn, while and Cd and Pb are usually very low. Cu concentrations are higher in the finer grain size classes ($2 > s \geq 1$ mm) than in the coarser ones, as already seen in [26].

Table 5 reports the global mass balance we measured in steam washing treatments, in terms of (i) dissipated steam (i.e., dispersed in the environment. This fraction can be recovered up to ~80%; we do not discuss this point as it strays off the general purpose of the present work); (ii) retained water (i.e., adsorbed by the BA surface); (iii) wastewater (i.e., water collected from trickling across BA after condensation, and giving a leachate); (iv) weight loss (i.e., difference in mass between treated and untreated BA).

Table 5. Mass balance of the steam washing treatment referred to the three grain size classes investigated. The weight loss refers the BA weight difference after and before treatment; retained water, dissipated steam and wastewater fractions are referred to the initial water balance. Weight loss is expressed on dry weight.

Grain Size BA	Time (s)	Retained Water (wt%)	Dissipated Steam (wt%)	Wastewater (wt%)	Weight Loss (wt%)
≥4.75 mm	240	3	91	6	0.4
4.75 mm > $s \geq 2$ mm	600	2	85	13	5
2 mm > $s \geq 1$ mm	600	13	75	12	10

We compare the retained water figures of the BA classes having $s \geq 4.75$ and $2 \leq s < 4.75$ mm, neglecting the differences in terms of surface tensions [41] at the interface solid–liquid–vapor. Leaving aside any claim of precision, we extrapolate the retained water of BA ($s \geq 4.75$ mm) to 600 s. In doing so, we obtain a negative and unrealistic value, due to low accuracy, which nevertheless

suggests a remarkably smaller figure than BA ($4.75 > s \geq 2$ mm), i.e., 2 wt%. This result is consistent with BA ($4.75 > s \geq 2$ mm) exhibiting a larger specific surface area than BA ($s \geq 4.75$ mm). We stress the crucial role played by the particle size, which reflects not only a purely dimensional aspect, but accounts also for deeper differences between the materials involved (large BA are mainly composed of quasi-inert ceramic/glass fragments, whereas small BA also include new products formed upon heating).

In the case of BA (s < 1 mm), steam washing is difficult, as it induces flocculation phenomena that require additional dispersants to properly counterbalance agglomeration (Na-silicate ~0.1 wt%; Na-carbonate ~0.02 wt%; phosphonate ~0.06 wt%). Small particles have a large specific surface area [26], which makes them active exchangers and affects the ionic strength of the resulting solution (~45 mmol/L), thus engendering flocculation [42].

3.2. Carbonation

Carbonation was explored on BA ($2 > s \geq 1$ mm) and BA (s < 1 mm), namely the cases for which steam washing is not fully effective, as discussed above. Only the most salient results for BA ($s < 1$ mm) are set out in Table 6; the results achieved for BA ($2 > s \geq 1$ mm) are shown by Table S2, in the Supplementary Materials. As for BA ($2 > s \geq 1$ mm), carbonation is successful in reducing Cu concentration below the legal limit ($T = 60$ °C; $P = 2$ bar; $t = 60$ min), although it fails in curbing sulphate and chloride sufficiently.

Table 6. Carbonation of BA $s < 1$ mm ($T = 6, 20, 60$ °C; $t = 60, 180$ min; L/S = 0.3), $P_{CO_2} = 2$ bar. Standard deviations are set out. Concentration values are expressed in mg/L.

Time, Temperature	Cl^-	SO_4^{2-}	NO_3^-	Ni	Zn	Ba	Cd	Co	Cr	Cu	Pb
Untreated, 20 °C	1223	378	1.15	0.063	0.065	0.068	0.118	0.148	0.15	3.065	0.02
St. Dev. $s < 1$ mm	124.1	51	1.04	0.01	0.044	0.039	0.013	0.021	0.014	0.093	0.008
60 min, 20°C	1185	354	0.63	0.056	0.107	0.133	0.142	0.156	0.135	0.786	0.097
St. Dev. $s < 1$ mm	120.8	24.2	0.05	0.001	0.013	0.012	0.041	0.007	0.014	0.118	0.028
60 min, 60 °C	792	152	3.48	0.002	0.006	0.067	0.003	0.001	0.006	0.483	0.001
St. Dev.	2	1	0.03	0.001	0.012	0.006	0.006	0.001	0.006	0.042	0.008
180 min, 20 °C	1116	253	0.57	0.007	0.11	0.046	0.001	0.002	0.02	0.045	0.003
St. Dev.	210	68	0.05	0.005	0.009	0.075	0	0.001	0.01	0.005	0.002
Italian legal limit values (mg/L)	100	250	50	0.01	3	1	0.005	0.25	0.05	0.05	0.05

Carbonation treatments yield unambiguously decreasing trends of all contaminants upon increasing temperature and/or time. Chlorides and sulfates remain above legal limit values, whereas Cu suffers a drastic reduction and after 180 min, treatment lies below the legal limits.

Using TGA-FTIR, (Figure 6) we estimated the sequestered CO_2 amount, by comparing the weight change of carbonated BA with respect to the pristine bottom ash samples, and obtained figures in the range 3.7–5.6 wt%, with an average of ~5 wt%.

XRPD measurements and Rietveld refinements, carried out on all treated and untreated samples, yield a slight average increase in calcite of ~3 wt% due to carbonation (Figure 7). Therefore, it can be concluded that ~25–30 wt% of the provided CO_2 has been sequestered into crystalline calcite. ^{13}C MAS SSNMR spectroscopy [43,44] exhibits signals in the carbonate region, i.e., 165–170 ppm, and the strongest peak at 168.2 ppm is attributable to calcite [45]. A remarkable increase of the calcite signal intensity is visible in the treated samples (Figure 8).

On the one hand, XRPD and SSNMR (Figure 8) agree to attribute to calcite a prominent role in sequestering CO_2; on the other hand, both methods show a broadening of the calcite signals, thus suggesting occurrence of low crystallinity/amorphous structures and carbonate other than calcite. This is in keeping with the composition provided by [26] for BA ($s < 1$ mm), in which the following molar ratios Pb/Ca = 3.5×10^{-4}, Zn/Ca = 1.4×10^{-2}, Cu/Ca = 7.5×10^{-3}, confirm that Ca-carbonate is by far the most likely to form. The low leaching of Cu-Ni-Cr-Pb-Cd [28,46] in the observed pH range (8–8.5), the stability of carbonate in a CO_2-saturated solution [47] and the low solubility products

of transition metal carbonate (~10^{-9}–10^{-14}, copper-lead carbonate) point to heavy metals entering carbonate structures that exhibit different degrees of crystallinity.

Carbon EDS maps (~25 10^6 analysis points) recorded by SEM-EDS (Figure 9) from a suite of treated versus untreated BA grains yield an average increase of carbon (ΔC) from 8.6(±3) to 15.7(±5) wt%. The "flat" gaussian distribution of ΔC (μ = 7.1, σ = 6.8) implies ΔC > 0 with a probability larger than 83.7%, thus hinting at carbonation processes spread across the sample's surface.

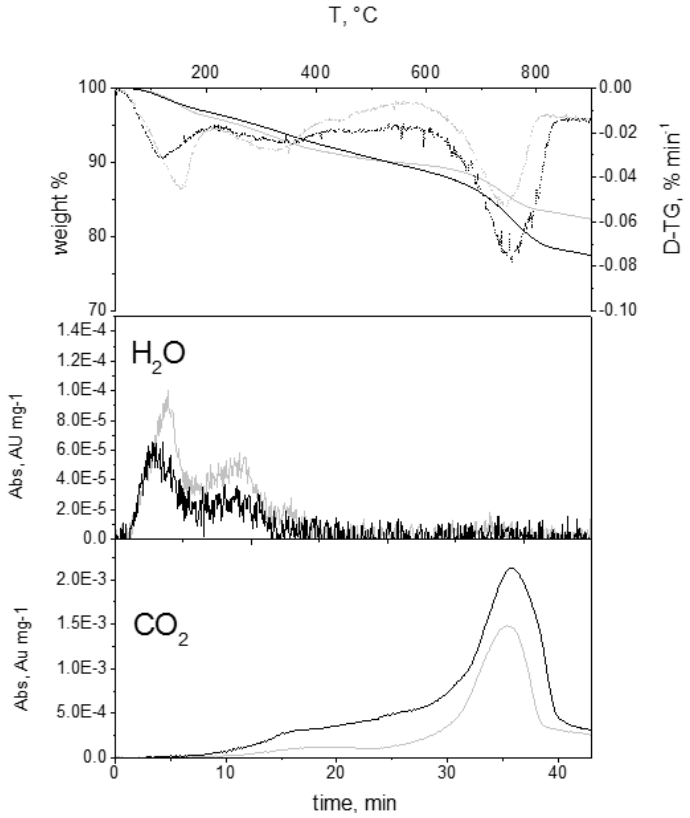

Figure 6. BA with $s < 1$ mm. Grey lines: BA not treated; black lines: BA carbonated; Solid lines: TG; Dashed lines: derivatives recorded as function of temperature for untreated sample (grey) and carbonated sample (black). The case of BA with $s < 1$ mm, at $T = 60$ °C, $P_{CO_2} = 2$ bar, $t = 60$ min and a water content of L/S = 0.3 is shown, by way of example. In the temperature range from 30 to 540 °C, both samples exhibited qualitatively similar thermal behavior, characterized by the release of adsorbed H_2O and small amounts of CO_2. At higher temperatures, an important weight loss occurs for both samples (~747 °C), accompanied by a release of CO_2, which can be ascribed to the decomposition of carbonate. The weight loss observed in the temperature range between 560 and 840 °C for untreated (~6.5 wt%) and carbonated BA (~11.5 wt%) yields a net sequestered CO_2 amount as large as approximately 4–5 wt%.

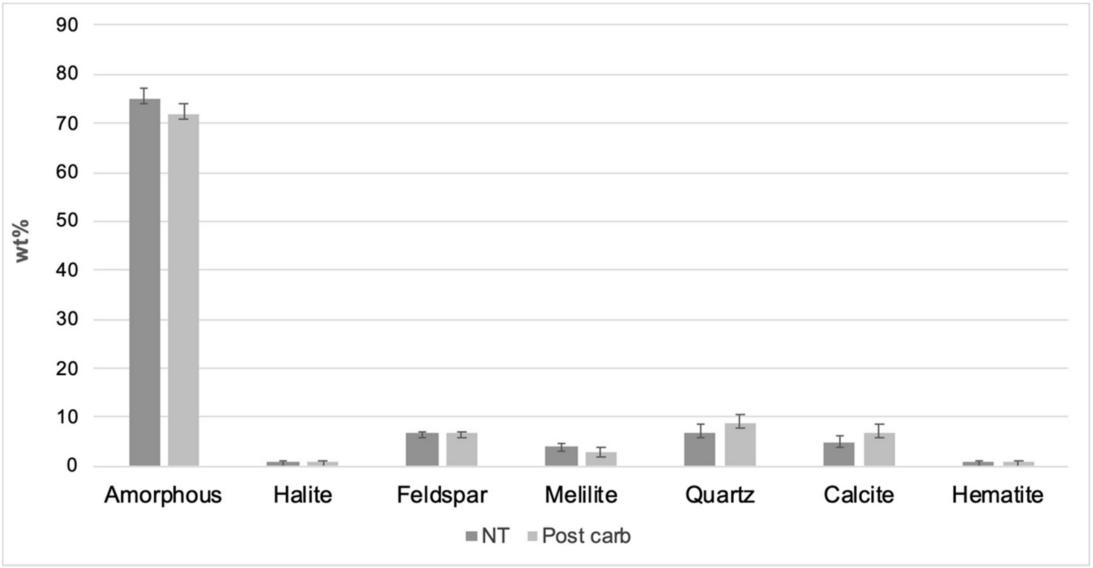

Figure 7. Average phase compositions of treated (post carb) versus non treated (NT) samples, inferred by X-ray Powder Diffraction on BA ($s < 1$ mm). Treatment conditions: P_{CO_2} = 2 bar, L/S = 0.3, T = 20 °C and time = 180 min. The results shown are obtained as the average of five independent samplings and related XRPD data collections for either sample.

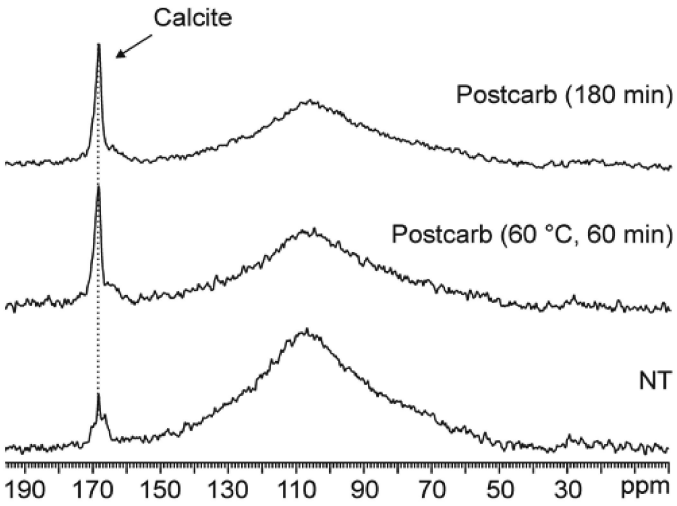

Figure 8. 13C (150 MHz) MAS spectra of untreated (NT) and two carbonated, T = 60 °C, P_{CO_2} = 2 bar, t = 60 min and L/S = 0.3, (Postcarb) BA samples ($s < 1$ mm), acquired at room temperature at a spinning speed of 20 kHz. Following a convention of NMR data, the Y axis, which reports an arbitrary unit, is missing. The broad peak at about 108 ppm is a spurious signal due to the rotor background.

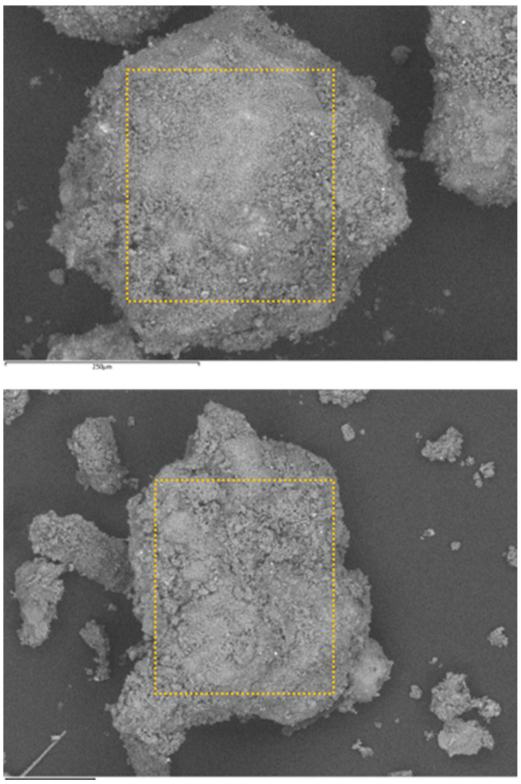

Figure 9. SEM images of carbonated BA samples (s < 1 mm). SEM-EDS observations show BA grains < 1 mm after treatment, highlight the complex and aggregate structure of such particles. (Experimental conditions: W filament, accelerating voltage 15 kV, working distance 10 mm, standard probe current, magnification 180×, top, and 220×, bottom).

4. Conclusions

The study demonstrates that steam washing allows a successful treatment of BA. This novel approach leads to a decrease of chlorides and heavy metals leaching from treated BA, to under the Italian legal limits. Analyses of the solid and liquid residues resulting from steam washing point to the occurrence of both a mild dissolution of the most soluble components (chlorides and sulfates) and a mechanical removal of the finer dust adherent to the larger particles' surface. This method has been tested by employing a steam similar to that coming from the circuit dedicated to the production of electricity used in urban district heating; this energy resource is always available in all waste-to-energy plants equipped with a cogeneration system.

Particle size separation has been proven useful to tune the time of steam exposure for both maximizing the efficacy of the treatment and minimizing steam usage. The BA fraction with $s \geq 4.75$ mm (36 wt%) requires 240 s to reach neutralization, while the intermediate fraction with $4.75 > s \geq 2$ mm (24 wt%) needs a longer exposure, up to 600 s. Chlorides and sulfates, as well as heavy metals, are reduced under the legal limits, only by steam washing. Thus, these BA fractions can be considered suitable for reuse.

BA ($2 > s \geq 1$ mm) is positively treated by steam washing (600 s) for chloride and sulfate, reduced up to 95%, whereas carbonation is successful in reducing the leaching of heavy metals, especially copper, which decreases by 90%, being under the legal limit. Therefore, this fraction could be recovered by a combination of steam washing and accelerated carbonation. Steam washing affects BA by a combination of mild dissolution and mechanical removal of the fine dust adherent to the surface of the particles, demonstrated by both the XRPD and SEM analysis on the solid residue of the wastewater, and the chemical composition of the wastewater.

Steam washing cannot be conveniently employed for very fine BA ($s < 1$ mm), because the large surface area induces flocculation phenomena that require dispersants. Carbonation, in turn, allows the reduction of heavy metals to below the legal limits, but it fails to sufficiently curb chloride and sulfate. On the BA fraction with $s < 1$ mm, accelerated carbonation is effective in reducing heavy metals after 180 min of treatment (P_{CO_2} = 2 bar, T = 20 °C, L/S = 0.3), especially copper, which is reduced under the legal limit. Chlorides and sulfates yet remain over the legal value. XRPD, TGA coupled with FTIR, and NMR analyses show that carbonation mainly takes place in terms of formation of carbonate compounds, which are represented by calcite (major phase) with a low degree of crystallinity. XRPD measurements and Rietveld refinements, carried out on all treated and untreated samples, yield a slight average increase in calcite of ~3 wt%, due to carbonation. A remarkable increase of the calcite signal intensity is also visible by ^{13}C MAS SSNMR spectroscopy in the treated samples. XRPD and SSNMR agree to attribute to calcite a prominent role in sequestering CO_2; both methods show a broadening of the calcite signals, thus suggesting occurrence of low crystallinity/amorphous structures and carbonate other than calcite.

These results suggest that further investigations of physical and chemical parameters controlling steam washing will consolidate this method for the improvement of the environmental compatibility of coarse bottom ashes. The finer fractions of BA require further studies on their stabilization aimed at reuse and environmental suitability.

Supplementary Materials: The following are available online at http://www.mdpi.com/2071-1050/12/22/9461/s1, Figure S1: Particle size distribution of BA investigated in the present study; Figure S2: Conductivity (µS/cm) versus time (s) of leachates of BA after steam washing treatments; Table S1: PHREEQC modelling results of BA ($2 > s \geq 1$ mm) wastewater solution, using MINTEQ v.4 database; Table S2: Carbonation of BA $2 > s \geq 1$ mm (T = 60 °C; t = 60, L/S = 0.2), P_{CO_2} = 2 bar.

Author Contributions: Conceptualization, E.D.; methodology, C.C., E.D., A.P. and G.M.; validation, C.C., E.D., D.B. and Q.W.; formal analysis, C.C. and D.B.; investigation, C.C., E.D., D.B., G.C., L.P., C.B., Q.W., I.C. and F.T.; resources, C.C., E.D., D.B., C.B., Q.W. I.C., F.T. and R.B.; data curation, C.C.; writing—original draft, C.C. and A.P.; writing—review and editing, C.C., E.D., D.B., C.B., L.P., A.P. G.M. and E.B.; visualization, C.C.; supervision, E.D., G.M. and A.P.; project administration, A.P.; funding acquisition, A.P. and G.M. All authors have read and agreed to the published version of the manuscript.

Funding: The present study (AP) has been partly funded by the project PRIN 2017-2017L83S77 (Italian Ministry for Education, University and Research, MIUR) and by TRM (IREN Group).

Acknowledgments: The paper benefited from the English language editing provided by Barbara Galassi (Brighton, UK). We also thank for their collaboration ETG s.r.l. (Montiglio, Asti, Italy) and Maina G. s.r.l. (Pecetto, Turin, Italy).

Conflicts of Interest: The authors declare no conflict of interest. The funders had no role in the design of the study; in the collection, analyses, or interpretation of data; in the writing of the manuscript, or in the decision to publish the results; they provided the samples only.

References

1. CEWEP. Bottom ash Factsheet 2017. Available online: http://www.cewep.eu/wp-content/uploads/2017/09/FINAL-Bottom-Ash-factsheet.pdf (accessed on 12 November 2020).
2. Zhu, W.; Teoh, P.J.; Liu, Y.; Chen, Z.; Yang, E.-H. Strategic utilization of municipal solid waste incineration bottom ash for the synthesis of lightweight aerated alkali-activated materials. *J. Clean. Prod.* **2019**, *235*, 603–612. [CrossRef]
3. Chimenos, J.M.; Fernández, A.I.; Miralles, L.; Segarra, M.; Espiell, F. Short-term natural weathering of MSWI bottom ash as a function of particle size. *Waste Manag.* **2003**, *23*, 887–895. [CrossRef]
4. Chimenos, J.M.; Segarra, M.; Fernández, M.A.; Espiell, F. Characterization of the bottom ash in municipal solid waste incinerator. *J. Hazard. Mater.* **1999**, *64*, 211–222. [CrossRef]
5. Forteza, R.; Far, M.; Seguí, C.; Cerda, V. Characterization of bottom ash in municipal solid waste incinerators for its use in road BAe. *Waste Manag.* **2004**, *24*, 899–909. [CrossRef] [PubMed]
6. Šyc, M.; Krausová, A.; Kameníková, P.; Šomplák, R.; Pavlas, M.; Zach, B.; Pohořelý, M.; Svoboda, K.; Punčochář, M. Material analysis of Bottom ash from waste-to-energy plants. *Waste Manag.* **2018**, *73*, 360–366. [CrossRef] [PubMed]

7. Joseph, A.M.; Snellings, R.; Van den Heede, P.; Matthys, S.; De Belie, N. The Use of Municipal Solid Waste Incineration Ash in Various Building Materials: A Belgian Point of View. *Materials* **2018**, *11*, 141. [CrossRef] [PubMed]
8. Lam, C.H.K.; Ip, A.W.M.; Barford, J.P.; McKay, G. Use of Incineration MSW Ash: A Review. *Sustainability* **2010**, *2*, 1943–1968. [CrossRef]
9. Hjelmar, O.; Holm, J.; Crillesen, K. Utilisation of MSWI bottom ash as sub-BAe in road construction: First results from a large-scale test site. *J. Hazard. Mater.* **2007**, *139*, 471–809. [CrossRef]
10. Sorlini, S.; Collivignarelli, M.C.; Abbà, A. Leaching behaviour of municipal solid waste incineration bottom ash: From granular material to monolithic concrete. *Waste Manag. Res.* **2017**, *35*, 978–990. [CrossRef]
11. Silva, R.V.; de Brito, J.; Lynn, C.J.; Dhir, R.K. Environmental impacts of the use of bottom ashes from municipal solid waste incineration: A review. *Resour. Conserv. Recycl.* **2019**, *140*, 23–35. [CrossRef]
12. Kavouras, P.; Kaimakamis, G.; Ioannidis, T.A.; Kehagias, T.; Komninou, P.; Kokkou, S.; Pavlidou, E.; Antonopoulos, I.; Sofoniou, M.; Zouboulis, A.; et al. Vitrification of lead-rich solid ashes from incineration of hazardous industrial wastes. *Waste Manag.* **2003**, *23*, 361–371. [CrossRef]
13. Xiao, Y.; Oorsprong, M.; Yang, Y.; Voncken, J.H.L. Vitrifcation of bottom ash from a municipal solid waste incinerator. *Waste Manag* **2008**, *28*, 1020–1026. [CrossRef] [PubMed]
14. Stabile, P.; Bello, M.; Petrelli, M.; Paris, E.; Carroll, M.R. Vitrification treatment of municipal solid waste bottom ash. *Waste Manag.* **2019**, *95*, 250–258. [CrossRef] [PubMed]
15. Alam, Q.; Schollbach, K.; Florea, M.V.A.; Brouwers, H.J.H. Investigating washing treatment to minimize leaching of chlorides and heavy metals from MSWI bottom ash. In Proceedings of the 4th International Conference on Sustainable Solid Waste Management, Limassol, Cyprus, 22–25 June 2016.
16. Alam, Q.; Florea, M.V.A.; Schollbach, K.; Brouwers, H.J.H. A two-stage treatment for Municipal Solid Waste Incineration (MSWI) bottom ash to remove agglomerated fine particles and leachable contaminants. *Waste Manag.* **2017**, *67*, 181–192. [CrossRef]
17. Alam, Q.; Lazaro, A.; Schollbach, K.; Brouwers, H.J.H. Chemical speciation, distribution and leaching behavior of chlorides from municipal solid waste incineration bottom ash. *Chemosphere* **2020**, *241*, 124985. [CrossRef]
18. Asal, S.; Laux, S.J.; McVay, M.C.; Townsend, T.G. Blending organic material with municipal solid waste incinerator bottom ash to promote in-situ carbonation in road base. *Waste Manag. Res.* **2019**, *37*, 951–955. [CrossRef] [PubMed]
19. Lin, Y.C.; Panchangam, S.C.; Wu, C.H.; Hong, P.K.A.; Lin, C.F. Effects of water washing on removing organic residues in bottom ashes of municipal solid waste incinerators. *Chemosphere* **2011**, *82*, 502–506. [CrossRef]
20. Keulen, A.; van Zomeren, A.; Harpe, P.; Aarnink, W.; Simons, H.A.E.; Brouwers, H.J.H. High performance of treated and washed MSWI bottom ash granulates as natural aggregate replacement within earth-moist concrete. *Waste Manag.* **2016**, *49*, 83–95. [CrossRef]
21. Quek, A.; Xu, W.; Guo, L.; Wu, D. Heavy metal removal from incineration bottom ash through washing with rainwater and seawater. *Int. J. Waste Resour.* **2016**, *6*, 1–9. [CrossRef]
22. Šyc, M.; Simon, F.G.; Hykš, J.; Braga, R.; Biganzoli, L.; Costa, G.; Funari, V.; Grosso, M. Metal recovery from incineration bottom ash: State-of-the-art and recent developments. *J. Hazard. Mater.* **2020**, *393*, 122433. [CrossRef]
23. Funari, V.; Mantovani, L.; Vigliotti, L.; Dinelli, E.; Tribaudino, M. Geochemical and magnetic data on anthropogenic ashes from municipal solid waste incineration (MSWI). *Data Brief* **2020**, *31*, 105728. [CrossRef] [PubMed]
24. Funari, V.; Braga, R.; Bokhari, S.N.H.; Dinelli, E.; Meisel, T. Solid residues from Italian municipal solid waste incinerators: A source for "critical" raw materials. *Waste Manag.* **2015**, *45*, 206–216. [CrossRef] [PubMed]
25. Møller, H. Sampling of heterogeneous bottom ash from municipal waste-incineration plants. *Chemometr. Intell. Lab. Syst.* **2004**, *74*, 171–176. [CrossRef]
26. Caviglia, C.; Confalonieri, G.; Corazzari, I.; Destefanis, E.; Mandrone, G.; Pastero, L.; Boero, R.; Pavese, A. Effects of particle size on properties and thermal inertization of bottom ashes (MSW of Turin's incinerator). *Waste Manag.* **2019**, *84*, 340–354. [CrossRef]
27. Fernández Bertos, M.; Simons, S.J.R.; Hills, C.D.; Carey, P.J. A review of accelerated carbonation technology in the treatment of cement-BAed materials and sequestration of CO_2. *J. Hazard. Mater.* **2004**, *112*, 193–205. [CrossRef]

28. Van Gerven, T.; Van Keer, E.; Arickx, S.; Jaspers, M.; Wauters, G.; Vandecasteele, C. Carbonation of MSWI-bottom ash to decrease heavy metal leaching, in view of recycling. *Waste Manag.* **2005**, *25*, 291–300. [CrossRef]
29. Baciocchi, R.; Costa, G.; Lategano, E.; Marini, C.; Polettini, A.; Pomi, R.; Postorino, P.; Rocca, S. Accelerated carbonation of different size fractions of bottom ash from RDF incineration. *Waste Manag.* **2010**, *30*, 1310–1317. [CrossRef]
30. Nam, S.-Y.; Seo, J.; Thriveni, T.; Ahn, J.-W. Accelerated carbonation of municipal solid waste incineration bottom ash for CO_2 sequestration. *Geosystem Eng.* **2012**, *15*, 305–311. [CrossRef]
31. Pan, S.Y.; Chang, E.E.; Chiang, P.C. CO_2 capture by accelerated carbonation of alkaline wastes: A review on its principles and applications. *Aerosol Air Qual. Res.* **2012**, *2*, 770–791. [CrossRef]
32. Gualtieri, A. Accuracy of XRPD QPA using the combined Rietveld-RIR method. *J. Appl. Cryst.* **2000**, *33*, 267–278. [CrossRef]
33. Toby, B.H.; Von Dreele, R.B. GSAS-II: The genesis of a modern open-source all purpose crystallography software package. *J. Appl. Cryst.* **2013**, *46*, 544–549. [CrossRef]
34. Lin, W.Y.; Heng, K.S.; Nguyen, M.Q.; Ho, J.R.I. Evaluation of the leaching behavior of incineration bottom ash using seawater: A comparison with standard leaching tests. *Waste Manag.* **2017**, *62*, 139–146. [CrossRef] [PubMed]
35. Tiwari, M.K.; Bajpai, S.; Dewangan, U.K.; Tamrakar, R.K. Suitability of leaching test methods for fly ash and slag: A review. *J. Radiat. Res. Appl. Sci.* **2015**, *8*, 523–527. [CrossRef]
36. Yin, K.; Chan, W.P.; Dou, X.; Ren, F.; Chang, V.W.C. Measurements, factor analysis and modeling of element leaching from incineration bottom ashes for quantitative component effects. *J. Clean. Prod.* **2017**, *165*, 477–490. [CrossRef]
37. Ministerial Decree No. 186 dated 5 April 2006. Regulatory that modified Ministerial Decree dated 5 February 1998. *Official Gazette*, n. 115. 19 May 2006. (In Italian)
38. Parkhurst, D.L.; Appelo, C.A.J. *PHREEQC (Version 2.12.5.669)—A Computer Program for Speciation, Batch-Reaction, One-Dimensional Transport, and Inverse Geochemical Calculations*; U.S. Geological Survey: Reston, VA, USA, 2005.
39. Pitard, F.F. *Pierre Gy's Sampling Theory and Sampling Practice, Second Edition: Heterogeneity, Sampling Correctness, and Statistical Process Control*; CRC Press: Boca Raton, USA, 1993; p. 516.
40. Gauthier, T.D.; Hawley, M.E. Chapter 5—Statistical Methods. In *Introduction to Environmental Forensics*, 3rd ed.; Murphy, B.L., Morrison, R.D., Eds.; Academic Press: Waltham, MA, USA, 2015; pp. 99–148.
41. Bico, J.; Thiele, U.; Quere, D. Wetting of textured surfaces. *Colloids Surf. A Physicochem. Eng. Asp.* **2002**, *206*, 41–46. [CrossRef]
42. Cosgrove, T. *Colloid Science Principles, Methods and Applications*; Blackwell Publishing Ltd.: Hoboken, NJ, USA, 2005.
43. Wasylishen, R.E.; Ashbrook, S.E.; Wimperis, S. NMR of Quadrupolar Nuclei in Solid Materials. In *Encyclopedia of Magnetic Resonance*; Harris, R.K., Ed.; John Wiley & Sons Ltd.: Chichester, UK, 2012.
44. Harris, R.K.; Wasylishen, R.E.; Duer, M.J. *NMR Crystallography*; John Wiley & Sons Ltd.: Chichester, UK, 2009.
45. Nebel, H.; Neumann, M.; Mayer, C.; Epple, M. On the Structure of Amorphous Calcium Carbonate—A Detailed Study by Solid-State NMR Spectroscopy. *Inorg. Chem.* **2009**, *47*, 7874–7879. [CrossRef]
46. Dijkstra, J.J.; van der Sloot, H.A.; Comans, R.N.J. The leaching of major and trace elements from MSWI bottom ash as a function of pH and time. *Appl. Geochem.* **2006**, *21*, 335–351. [CrossRef]
47. Plummer, L.N.; Busemberg, E. The solubilities of calcite, aragonite and vaterite in CO_2-H_2O solutions between 0 and 90°C, and an evaluation of the aqueous model for the system $CaCO_3$-CO_2-H_2O. *Geochim. Cosmochim. Acta* **1982**, *46*, 1011–1040. [CrossRef]